From fission to scattering in the $^{100}Mo(18.7\ MeV/u) + ^{100}Mo$ reaction within a microscopic dynamic approach

F. Haddad, G. Royer, F. Sébille and B. Remaud
Laboratoire de Physique Nucléaire
IN2P3/CNRS et Université de Nantes
2, rue de la Houssinière - 44072 Nantes cedex 03- France

Abstract

A study of the transition from fission to deep-inelastic and quasi-elastic reactions in heavy ion collisions at intermediate energies is performed in the framework of a microscopic semi-classical one-body approach. The full ensemble technique is used to solve the Landau-Vlasov transport equation including a Uehling-Uhlenbeck collision term. A qualitative as well as quantitative study of phenomena occuring in this energy range is carried out and comparisons are made with experimental results focusing on the $Mo+Mo$ reaction at 18.7 MeV/u. On the ground of dynamical information given by the microscopic approach, an investigation of the sequential production of fragments is realized within a complementary analysis based on the macroscopic liquid-drop model approach.

1. Introduction

Since accelerators of heavy ions at intermediate energy are available, experimentalists have accumulated data proving the existence at these energies of a broad variety of processes like fusion, fission, evaporation, fragmentation, deep-inelastic regime,.... Theoretically, a great effort has been devoted to these complex dynamic processes during the last ten years introducing transport theories [1-6] and specially the Vlasov equation supplemented by the introduction of a collision term taking into account the two-body residual interactions. Many theoretical studies based on these approaches exist for rather short time mechanisms such as formation of hot excited nuclei, flow, fragmentation,... On the other hand, there is a lack of information on long time processes such as hot fission due to computing time required to simulate this kind of phenomena and problems of numerical accuracy. However, first attempts to induce fission of an isolated nucleus have been done using momentum fields [7,8] or rotational fields [9].

In the present paper, a detailed study of a collision between two heavy ions is realized for several impact parameters. The purpose is to perform a theoretical investigation in the framework of the Landau-Vlasov equation to describe the complete or incomplete fusion of two incoming nuclei in relatively central collisions followed by the hot fission of the unstable formed system. More generally, we study the transition from fission to deep-inelastic regime and quasi-elastic reactions with increasing impact parameters. To follow nuclear reactions on longer time, the code has been vectorized and new computer generation has been used. That has also allowed to better describe the distribution function improving the sampling of the phase-space. There are several advantages to use this microscopic approach taking into account both mean field and residual interactions. All phenomena taking place in heavy-ion reactions may be described with the same input parameter set and collective properties derived directly from the individual nucleon motion. Escape of nucleons occurs naturally which contributes to desexcite the hot nuclear system and to lower the rotational energy [10,11]. This evaporation tends to favor some exit channels and to inhibit some other ones. Another important feature is that there is no shape constraint and the system is free to investigate any fission valley.

In this paper, the well experimentally known $^{100}Mo(18.7MeV/u) +^{100} Mo$ reaction [12-14] has been selected. The model is briefly reviewed in sect. 2 and the behaviour of a nucleus on long time is displayed in sect.3. In sect. 4 simulations of the projected density profiles are visualized as a function of the impact parameter and our results are compared with experimental data. The Wilczynski plots (total kinetic energy versus polar angle and TKE versus mass fragments) are particularly investigated. Later on, signatures of the transition from fission following incomplete fusion to deep-inelastic regime are shown by the fast change of behaviour of several observables. In sect. 5 the dynamics of the fission process is studied. Finally, in sect. 6 the ternary hot fission which is an important part of the total cross section (20%) at this energy is described within a macroscopic dynamical model.

2. Description of the semi-classical model

The Landau-Vlasov semi-classical approach is based on the Vlasov equation for the one-body distribution function $f(\vec{r},\vec{p},t)$ and a collision term taking into account the residual interaction :

$$\frac{\partial f}{\partial t} + \{f, H\} = I_{coll}(f). \tag{2.1}$$

$H(\vec{r},\vec{p})$ is the Hartree-Fock Hamiltonian and $\{\ \}$ stands for the Poisson bracket. I_{coll} is the Uehling-Uhlenbeck collision term [15]. It has been compared with analytical solutions in ref. 16). $f(\vec{r},\vec{p},t)$ can be interpreted as the probability to find a particle in a particular point of the phase space, at the instant t. This equation is solved by projection on a continuous basis of frozen coherent states which have gaussian shapes with fixed widths in $\vec{r}$ and $\vec{p}$ spaces. The centres of these gaussians move according to Ehrenfest equations. One of the interests of this coherent state basis is its ability to describe the diffusivity of the nuclear surface beyond the

classical turning point.

The effective potential including the incompressibility modulus degree of freedom and nucleon-nucleon collision cross section in nuclear matter are the main ingredients of this model. Due to no definitive conclusion on the behavior of the nucleon-nucleon cross section in the nuclear medium, the free one with its isospin and energy dependence has been kept [17]. The mean field is taken as the soft local Skyrme interaction (Zamick prescription) with an extra isospin dependent term [18]. It reads :

$$U_q(\rho,\xi) = t_0\frac{\rho}{\rho_0} + t_3(\frac{\rho}{\rho_0})^{1+\nu} + c\frac{\xi^2}{\rho_0^2} + 4c\frac{q\rho\xi}{\rho_0^2}, \tag{2.2}$$

where $q = \frac{1}{2}$ for neutrons and $-\frac{1}{2}$ for protons. $\rho(\vec{r})$ is the local density :

$$\rho(\vec{r}) = \rho_n(\vec{r}) + \rho_p(\vec{r}) \tag{2.3}$$

and

$$\xi(\vec{r}) = \rho_n(\vec{r}) - \rho_p(\vec{r}). \tag{2.4}$$

The parameters values are :

$$t_0 = -356\ MeV \quad ,t_3 = 303\ MeV, \quad \nu = \frac{1}{6}\ and \quad c = 20\ MeV. \tag{2.5}.$$

c is related to the volume-symmetry coefficient J of the mass formula. This effective interaction has been introduced in the present study to better reproduce the nucleon exchange and the large neutron-proton asymmetry of this system. Indeed, the asymmetry coefficient (N-Z)/A reaches 0.16 for such a nucleus and the influence of the isospin term plays an important role in the research of the ground state which is performed self-consistently as in Hartree-Fock calculations.

3. Time dispersion of basic observables

The time requisite to construct the collective process of fission from the intrinsic microscopic degrees of freedom is long ($\sim 10^{-21} - 10^{-20} s$) comparatively to other nuclear phenomena such as fusion, fragmentation... Our semi-classical description of heavy-ion dynamics has proved its ability to describe fast nuclear processes. Before going further, the stability of an isolated ^{100}Mo nucleus on a long period is investigated in figure 1. The nucleus, intially in the ground state, evolves freely in its self-consistent mean field. Due to sampling of the phase-space, spurious nucleon evaporation appears. In the left upper part, a quantitative evaluation of this evaporation of nucleons is given. For short time this phenomenon does not exist anyway but with increasing evolution time it grows and reaches 4.8% of the total mass at $t = 1000$ fm/c. Consequently, for very long time, this implies a small underestimation of the fragment mass but the nature of the reaction is not strongly affected and the calculated main features are reliable.

In the right upper part of the figure 1, η is the quadrupole moment of the momentum distribution relatively to the fixed p_z axis :

$$\eta(t) = \int \frac{d^3\vec{p}d^3\vec{r}}{h^3} f(\vec{r},\vec{p},t)(2p_z^2 - p_x^2 - p_y^2). \tag{3.1}$$

η oscillates around zero which means that the nucleus remains cold after a long time.

The time evolution of the intrinsic angular momentum is described in the third part of the figure. The nucleus is simulated by a distribution of 6000 gaussians and the initial non zero value of the angular momentum comes from the inhomogeneity of this incomplete basis of coherent states. The L values keep close to the initial value.

The geometric quadrupole moment relative to the principal axes X,Y,Z of the matter distribution is shown in the last part of the figure :

$$Q(t) = \int \frac{d^3\vec{p}d^3\vec{r}}{h^3} f(\vec{r},\vec{p},t)(2Z^2 - X^2 - Y^2). \tag{3.2}$$

It is a measure of the distortion from the homogeneous spherical shape. The deviation from sphericity is small and does not increase with time. As a conclusion of this section, the incomplete character of the basis does not hinder the possibility to obtain quantitative information and weak indetermination on the observables gives confidence in the stability of the simulation even on a long time.

4. Simulation of the ^{100}Mo (18.7 MeV/u) + ^{100}Mo reaction

This nuclear system is well known experimentally [12-14] in an energy range between 12 MeV/u to 25 MeV/u. The importance of computing time to simulate a reaction at different impact parameters restricts us to select only one incident energy value (18.7 MeV/u). In this energy range, the system never goes through the spinodal zone and the fragments are heavy enough to legitimate the mean field approach. Binary fission following incomplete fusion is expected to be the most probable decay channel in relatively central collisions while ternary events ($\simeq$ 20% of the total cross-section) appear for more peripheral collisions. For this $^{100}Mo + ^{100}Mo$ reaction at 18.7 MeV/u, we have performed Landau-Vlasov calculations for a large family of impact parameters in order to investigate most of the experimental situations. For a given initial impact parameter two Mo nuclei in their ground state are boosted and their evolution is followed during 1000 fm/c. In the figure 2, the time evolution of the projected density on (x,z) plane is shown for impact parameters varying from 2 fm to 10 fm. The horizontal axis z corresponds to the beam direction and the x axis indicates the impact parameter. The time (fm/c unit) is given in the right upper corner of each panel. This representation allows a first rapid over-all view of the reaction mechanism as a function of the impact parameter. When the impact parameter decreases, a transition from positive to negative deflection angles occurs due to the increasing importance of the attractive nuclear potential which depends on the size of the overlap region. For $b \geq 7$ fm quasi-elastic and deep-inelastic processes take place. Reaction time is short and the two-body structure persists always during the reaction. For $b \leq 7$ fm the reaction time is larger, nucleon flow occurs in the nascent neck and leads to an excited nuclear system which subsequently undergoes fission. Scission happens after some 10^{-21}s which is consistent with usual estimates of the hot fission time. For $b = 4 - 5$ fm the fission is asymmetric. For $b = 2$ fm, the two incoming nuclei fuse and the system stays in an elongated state and rotates. Experimentally and for a close nuclear system, Gui et al [20] found recently that the fission time increases when the fission asymmetry decreases. They obtained a time order of 10^{-20}s for symmetric fission. We can't deal with such a long time and it might be possible that at $b = 2$ fm the elongated shape corresponds to a first stage of a symmetric fission.

In contrast to experiment, ternary fission events are not obtained within these Landau-Vlasov calculations. In sect. 6, this fact will be discussed and ternary fission will be investigated within a dynamical

macroscopic model.

4.1. Comparison with experimental data

The Landau-Vlasov simulation is based on full ensemble technique and gives only the mean value of the observables for each impact parameter and then, cannot reproduce the experimentally observed dispersion. In fig. 3 the experimental values [14] of the total kinetic energy of the fragments (two body events) are plotted versus the centre of mass scattering angle. Experimental data are corrected for background and efficiency set-up. The simulation results are represented for each impact parameter by a dot. The adopted procedure was to deduce the asymptotical values to take into account the infinite range of the Coulomb forces.

The highest TKE value corresponds to $b = 11$ fm and the lowest TKE values correspond to approximatively the Coulomb barrier obtained in the most central collisions. We observe an overall correct agreement for all impact parameters. The figure 4 shows the ability of the Landau-Vlasov approach to obtain the mean values of the fragment mass. For central impact parameters, two branches indicate asymmetrical fission events. The simulation compares suitably with experiment. These two comparisons with experimental data [14] allows to pursue a complete study focused on reaction mechanisms and their evolution as a function of the impact parameter.

4.2 Signature of a transition from inelastic scattering to fission regime

Contrarily to experimental data, in such a microscopic model the reaction plane and the impact parameter are known as well as the whole distribution of matter in the exit channel. In order to discriminate the impact parameters from the experimental results it is important to correlate them with observables predicted by the theoretical approach.

In figure 5, the TKE is displayed as a function of the impact parameter. The behaviour is linear for impact parameters higher or equal to 7 fm (see also ref. 21)). This result is interesting since it allows to determine basically b. This linear dependence disappears for more central collisions and the TKE reaches smoothly the pure Coulomb repulsion at the contact point. The reaction time (see figure 6) has been determined as the period from the ingoing channel to the scission process. In the two cases, the two fragments are too far to feel their mutual nuclear forces. It is tempting to fit the dots with two straight-lines of different slopes. The intersection point corresponds to an impact parameter value of 6.5 fm as deduced from the TKE.

In order to confirm the frontier between these two regions, a measure of the memory of the entrance channel distribution of matter is plotted in figure 7. This memory may be evaluated as the absolute difference n_{as} between the nucleons coming from the projectile and nucleons coming from the target inside the fragment divided by the fragment mass.

$$n_{as} = < |\frac{n_{p_i} - n_{t_i}}{A_i}| >_{i=1,2} \tag{4.1}$$

For impact parameters lower than 7 fm the memory is zero. For peripheral reactions, the asymmetry increases linearly with b. Then, these different data put forward a transition around 7 fm from deep-inelastic collisions to fast fission of a very excited nuclear system following incomplete fusion.

A last way to show the mixing effects is to focus on the nucleon distribution from the projectile during the reaction. The figure 8 provides the time evolution of projectile density profile in the reaction plane $(x, y = 0, z)$ for b = 4 fm and b = 10 fm. For the external impact parameter only a small part of the projectile is absorbed by the target during the reaction. In contrast, for b = 4 fm, the fusion mechanism

takes place. Progressively, the projectile nucleon distribution fills in the whole volume of the composite system. At 260 fm/c the projectile centre disappears. The distribution spreads and a fusion remnant appears. After 200 fm/c, two parts arise leading later to fission. Another interesting feature is the intrinsic angular momentum carried out by each outgoing fragment in the binary events (see figure 9). In very peripheral collisions the initial angular momentum is very high but the transfer is very weak due to a small overlap. This angular momentum transfer from the entrance channel to the fragments is maximal for impact parameter range from b = 8.5 fm to b = 6 fm and the fragment spin can reach values as high as 50 $\hbar$ for fragment mass number of about 90. For more central collisions intrinsic angular momenta of fragment remnants diminish with decreasing impact parameter till about 10$\hbar$. This corresponds to a fission following fusion process which leads to small fragment spins. This is due at once to smaller angular momenta available in the entrance channel, to a greater relaxation and evaporation. In the last part of the paper, the influence of the angular momentum on possible ternary fission will be discussed. Another discrimination can be made regarding the number of emitted nucleons prior to scission. In figure 10, this prescission evaporation is plotted distinguishing neutrons and protons. When the impact parameter decreases the intrinsic excitation energy and reaction time increase and the number of emitted nucleons is higher. This nucleon evaporation is essential to cool down the system. One always obtains more neutrons than protons as free particles.

5. Dynamical aspects of fission

In this section we focus on the fission process and particularly on its dynamical aspect. Let us recall that the present simulation allows the investigation of all the fission valleys without any shape constraint and the evaporation during the fission mechanism. Statically, fission process takes place when the excitation energy is larger than the static fission barrier height (quantum effects like tunneling are not present in this dynamical approach). To pass the barrier, the excited nucleus converts a part of its intrinsic energy to become deformed. In our prescription, the intrinsic energy is separated into two parts : the collective energy which characterizes a highly coherent motion and the thermal energy due to a ramdon motion which affects the surface properties of the momentum distribution. The thermal component plays an essential role for the evaporation process and a minor one in the lowering of the fission barriers. In contrast collective motion is the most important effect leading to fission. The collective effect is defined as :

$$E_{coll} = \frac{1}{2} m \int \rho(\vec{r}) v_{coll}^2(\vec{r}) d\vec{r}, \tag{5.1}$$

where the local density $\rho(\vec{r})$ is defined as :

$$\rho(\vec{r}) = \int f(\vec{r}, \vec{p}) \frac{d\vec{p}}{h^3}. \tag{5.2}$$

$v_{coll}(\vec{r})$ is the collective velocity field :

$$v_{coll}(\vec{r}) = \frac{1}{m\rho(\vec{r})} \int f(\vec{r}, \vec{p}) \vec{p} \frac{d\vec{p}}{h^3}. \tag{5.3}.$$

The system deformation can be analysed by following the time dependence of the spatial quadrupole moment. In order to remove rotational effects, the quadrupole moment has been determined along the principal axis of the deformed configuration. In figure 11, the variations of Q are plotted for three impact parameters. The system reaches the closest configuration to the sphere at about the same time in the three cases. For $b = 5$ fm, Q follows rapidly a parabolic behaviour indicating a linear increase of the elongation.

For b = 4 fm, the system needs more time to engage this process. For b = 2 fm, the system stays elongated till 1000 fm/c. In figure 12, the collective energy per nucleon is indicated, beginning when the equilibration is performed. Such a collective variable allows to take into account the particle emission. The mean density is also displayed. For b = 4 and 5 fm fission takes place and the collective energy diminishes till a minimum and later on, it increases. This is the inverted image of a dynamical barrier. The saddle point of which corresponds to the minimum of the collective energy. To determine the barrier height the equilibration time (close to 120 fm/c in all cases) serves as a reference. In the two cases the dynamic barrier height is about 55 MeV. These values are higher than the macroscopic and experimental ones but one must substract from these dynamic barrier heights the dissipated energy. In addition one has to remember the fact that the proximity forces between the surfaces in regard in the crevice separating the fragments still lower the barriers.

6. Ternary fission within a macroscopic dynamic model

The observed contribution of ternary events to the total cross section is approximatively 20%. At this relatively low energy it is not very likely that instantaneous disassembly in three fragments occurs. It is rather assumed that sequential ternary fragmentation in peripheral collisions is the dominant ternary process. Such three-body events are not obtained within the Landau-Vlasov approach. We must keep in mind that the Landau-Vlasov approach is a one-body theory giving only, for each impact parameter, the mean dynamical behaviour of nuclear systems. When different weighted processes are present for a given impact parameter the calculations describe only the dominant one. The limitation on the exploration time hinders also the realization of the two step process which is a more slow mechanism. In order to get some indications on this sequential fragment formation macroscopic approach has been used.

In the rotating liquid drop model including the nuclear proximity energy the intrinsic angular momentum plays an important role in moving the lower energy state towards deformed shape [22] and in decreasing the barrier height favorising the fission process. In figure 13, the l-dependent macroscopic barriers are plotted. In this mass range, nuclei are able to sustain angular momenta as high as $120\hbar$. In figure 9, the angular momenta of the remnant fragments are maximal between b = 6.5 fm and 8.5 fm encouraging fission and ternary events in this impact parameter range. The associated geometrical cross section of three-body events would be about 940 mb. This very rough high limit is compatible with the experimental one (600 mb) since other decay modes are ignored.

In figure 14, macroscopic fragmentation [23,24] into 2,3 and 4 spherical fragments are displayed. Q is the root mean square radius of the distribution of matter. The barrier height increases strongly with the number of fragments and the two-body barrier is at least twice lower than the other ones favourising this binary process. This is an other sign of the sequential nature of three-body events.

To check more precisely our hypothesis on the sequential origin of the three-body events, the binary fragmentation of the projectile in the target field has been studied within a macroscopic dynamic model [25,26]. In figure 15, the nature of the reaction is given as functions of the impact parameter, the projectile energy and the selected quasi-projectile. Four types of reactions appear. In the region a, there is no fragmentation, there are the quasi-elastic or deep-inelastic collisions. In the region b, the projectile breaks up and the two fragments are emitted. This is the sequential ternary fission region. In the region c, the projectile breaks up also but only the outer part (quasi-projectile) is emitted. The last region d corresponds to the fusion region. For all asymmetries the impact parameter range for three body events lies between 5 and 11 fm. For a given asymmetry the width of the b region is 4 fm but the mean value increases regularly with the quasi projectile mass. The range from 6.5 to 8.5 fm deduced from the Landau-Vlasov approach for this kind of ternary sequential hot fission is compatible with the b-window obtained from the macroscopic model. One must keep in mind that this macroscopic model doesn't take into account the evaporation degree of freedom, the target breaking and the friction forces act only on one part of the projectile. The introduction of all these effects would contribute to lower the width of the ternary sequential event area.

7. Conclusion

We have reported calculations on the dynamics of the $^{100}Mo(18.7\ \mathrm{MeV/u}) + ^{100}Mo$ reaction within the semi-classical Landau Vlasov approach including a Uehling-Uhlenbeck collision term. The model reproduces reasonably well the experimental data (Wilczynski plots) for two body events. For central impact parameter values, the fully damped nuclear system has forgotten the memory of the entrance channel. Dynamical barriers appear, the tops of which corresponding roughly to the scission point. The essential features of this scission point have been determined : total kinetic energy, angular momentum, asymmetry, number of evaporated nucleons and reaction time. For peripheral impact parameters, inelastic collisions are reproduced. The analysis of several observables emphasizes a transition region from deep-inelastic regime to hot fission processes occuring around b = 6.5 fm. Particularly, the spins of fragments are high in the impact parameter window between 6.5 fm and 8.5 fm. This window results from a competition between angular momentum transfer which increases when impact parameter decreases and evaporation, which lowers the angular momentum and becomes important for central collisions. These high angular momenta favor the fission process and should correspond to the sequential ternary event region. Macroscopic dynamic investigations confirm this hypothesis stressing that ternary events should take place in an intermediate impact parameter range.

References

1. H. Stocker and W. Greiner, Phys. Rep. 137 (1986) 277.

2. G. F. Bertsch and S. Das Gupta, Phys. Rep. 160 (1988) 189.

3. W. Cassing, K. Niita and S.J. Wang, Z. Phys. A 331 (1988) 439.

4. A. Bonasera, M. Colonna, M. Di Toro, F. Gulminelli and H.H. Wolter, Phys. Lett. B 244 (1990) 169.

5. J. Aichelin, Phys. Rep. 202 (1991) 233.

6. B. Remaud, C. Grégoire, F. Sébille and P. Schuck, Nucl. Phys. A 488 (1988) 423c.

7. Ch. Jung, W. Cassing, U. Mosel and R.Y. Cusson, Nucl. Phys. A 477 (1988) 256.

8. G. Royer, B. Remaud, F. Sébille and V. De La Mota, Phys. Rev. C 44 (1991) 2226.

9. F. Garcias, V. De La Mota, B. Remaud, G. Royer and F. Sébille, Phys. Lett. B 255 (1991) 311.

10. F. Garcias, V. De La Mota, B. Remaud, G. Royer and F. Sébille, Nucl. Phys. A 538 (1992) 275c.

11. B. Borderie, Ann. Phys. Fr. 17 (1992) 349.

12. S. Gralla et al, Phys. Rev. Lett. 54 (1985) 1898.

13. M. Petrovici, J. Albinski, R. Bock, R. Cusson, A. Gobbi, G. Guarino, S. Gralla, K.D. Hildenbrand, W.F.J. Müller, A. Olmi, H. Stelzer and J. Toke, Nucl. Phys. A 477 (1988) 277.

14. R.J. Charity et al, Z. Phys. A 341 (1991) 53.

15. C. Grégoire, B. Remaud, F. Sébille, L. Vinet and Y. Raffray, Nucl. Phys. A 465 (1987) 317.

16. G. Welke, R. Malfliet, C. Grégoire, M. Prakash and E. Suraud, Phys. Rev. C 40 (1989) 2611.

17. K. Hikasa et al, Phys. Rev. D 45 (1st) Part II (1992) III 85.

18. M. Farine, T. Sami, B. Remaud and F. Sébille, Z. Phys. A 339 (1991) 363.

19. B. Remaud, F. Sébille, C. Grégoire, L. Vinet and Y. Raffray, Nucl. Phys. A 447 (1986) 555c.

20. M. Gui et al, Texas A&M University report 93-01 (1993).

21. S. Hannuschke, W. Cassing, U. Mosel and K. Niita, Nucl. Phys. A 535 (1991) 120.

22. G. Royer and F. Haddad, Phys. Rev. C 47 (1993) 1302.

23. F. Haddad and G. Royer, J. Phys. G 18 (1992) L 153.

24. G. Royer, F. Haddad and J. Mignen, J. Phys. G 18 (1992) 2015.

25. G. Royer, Y. Raffray, A. Oubahadou and B. Remaud, Nucl. Phys. A 466 (1987) 199.

26. A. Oubahadou, R. Dayras and G. Royer, J. Phys. G 17 (1991) 1415.

Figure captions

Figure 1 : Time evolution of the main global characteristics for a ^{100}Mo nucleus in its ground state.

Figure 2 : Time evolution of the projected nuclear densities for increasing parameters. The time unit is fm/c. The horizontal and vertical coordinates are in fm. Contour lines are the same for all impact parameters and time. The absent curves correspond always to the highest densities.

Figure 3 : Comparison between the Wilczynski plot given the correlations between the kinetic energy (binary events) and the scattering angle in the centre-of-mass frame and the calculation results indicated by dots.

Figure 4 : Comparison between the experimental diffusion plot with respect to total kinetic energy and fragment mass and theoretical results. Each dot corresponds to a given impact parameter.

Figure 5 : Impact parameter dependence of the kinetic energy of the two fragments (in the centre of mass frame). Dots are calculations for several impact parameters. The dashed line gives the TKE corresponding to the Coulomb repulsion at the contact point of two ^{100}Mo nuclei.

Figure 6 : Reaction time versus impact parameter for binary events. Dots indicate the time deduced from the simulation.

Figure 7 : Asymmetry of the numbers of nucleons originating from the projectile and target in the outgoing fragments for binary events as a function of the impact parameter.

Figure 8 : Projected density profile of the projectile in the reaction plane for b = 4 and 10 fm. The time (fm/c unit) is given in the right upper corner of each panel. Density lines are normalized as in figure 2.

Figure 9 : Angular momentum of each fragment at the scission point as a function of the impact parameter.

Figure 10 : Number of emitted nucleons at the scission point as a function of the impact parameter.

Figure 11 : Time dependence of the quadrupole moment (relatively to the principal axis of the distribution of matter) for b = 2,4 and 5 fm.

Figure 12 : Collective energy per nucleon as a function of time from equilibration for b = 5, 4 and 2 fm. The density evolution is also plotted till the scission point(dashed curve).

Figure 13 : Macroscopic symmetric fission barriers for the $^{100}Mo + ^{100}Mo$ compound nucleus as a function of the distance r between the centres of the fragments and the angular momentum ($\hbar$ unit).

Figure 14 : Macroscopic fragmentation barriers into 2,3 or 4 fragments for the $^{100}Mo + ^{100}Mo$ compound

nucleus. The selected binary shape sequence is the family of elliptic lemniscatoids. The fragmentation into three or four fragments has been described from the contact point within equilateral triangle or tetrahedral configuration. The dashed curve corresponds to the longitudinal ternary fission leading to three aligned equal tangent spheres.

Figure 15 : Dependence of the reaction types on the impact parameter and the projectile energy for the $^{100}Mo+^{100}Mo$ system. The emitted quasi-projectile is indicated in each panel. The four domains a,b,c and d are defined in the text.

Figure 1

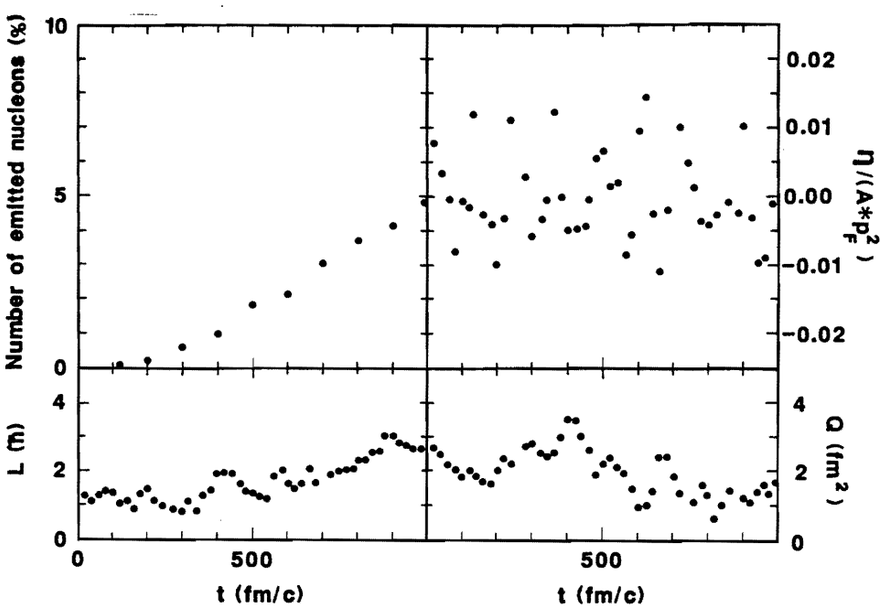

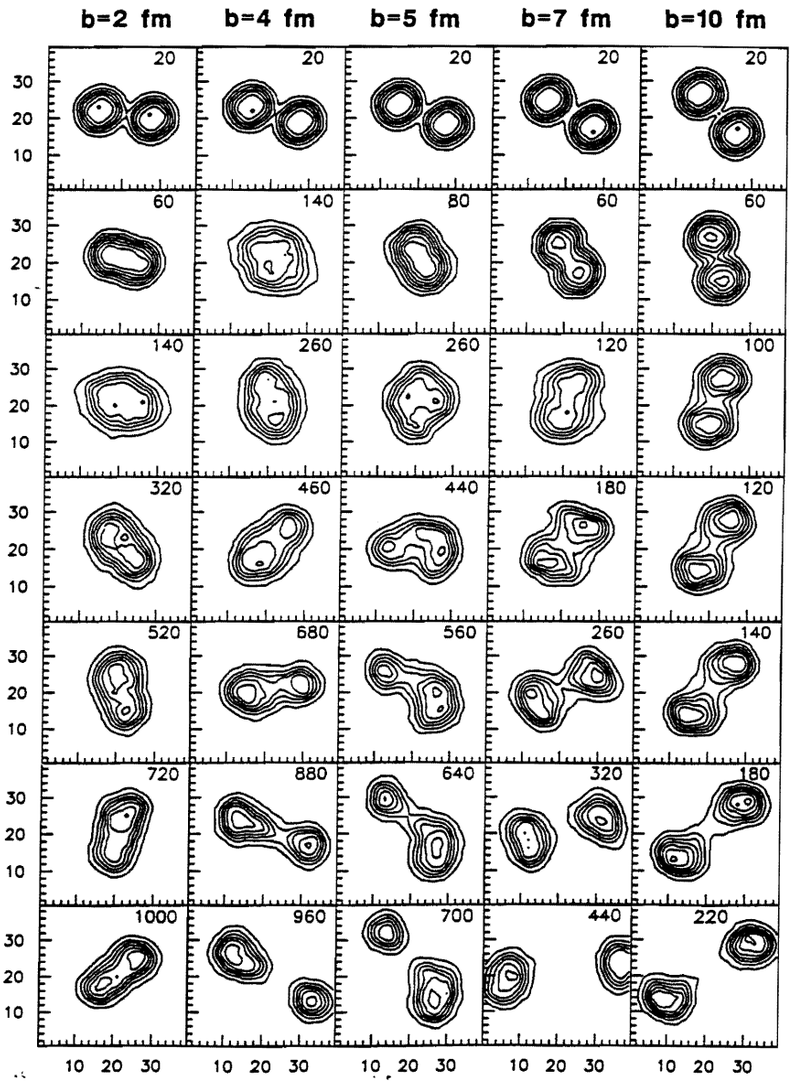

Figure 2

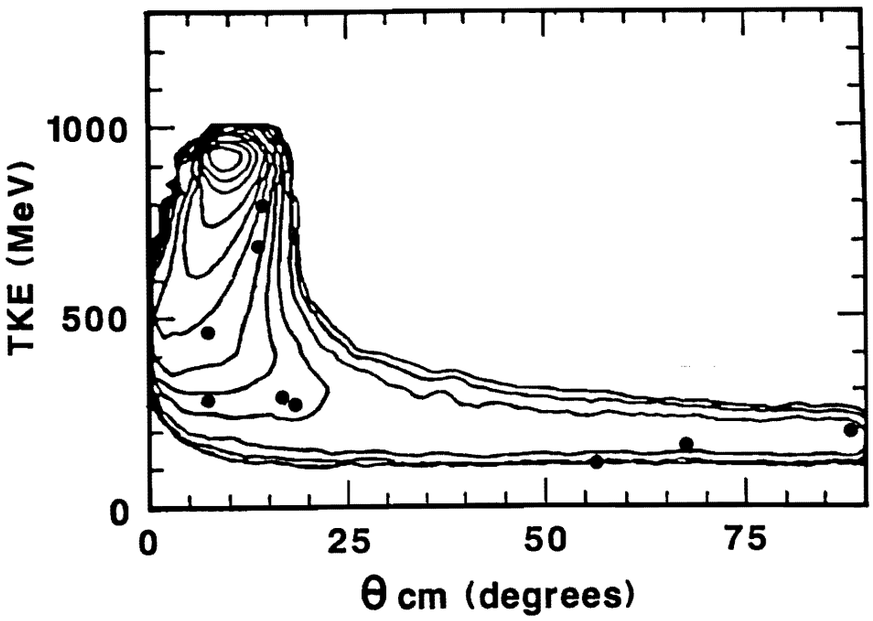

Figure 3

Figure 4

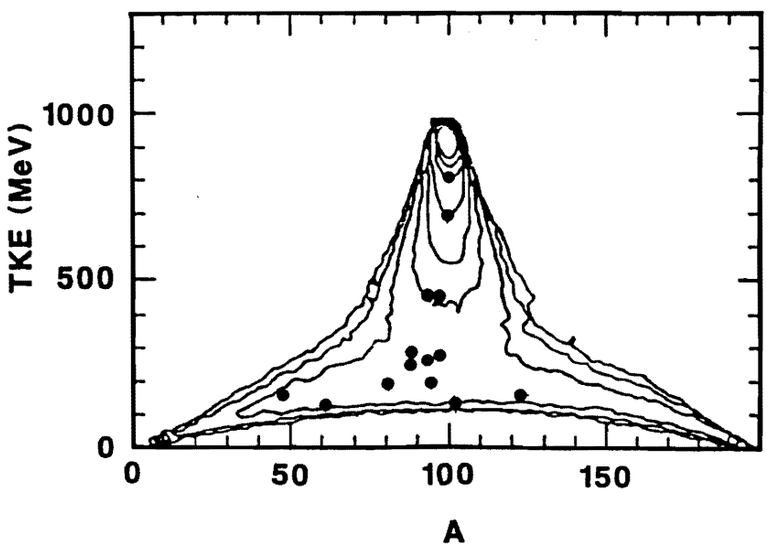

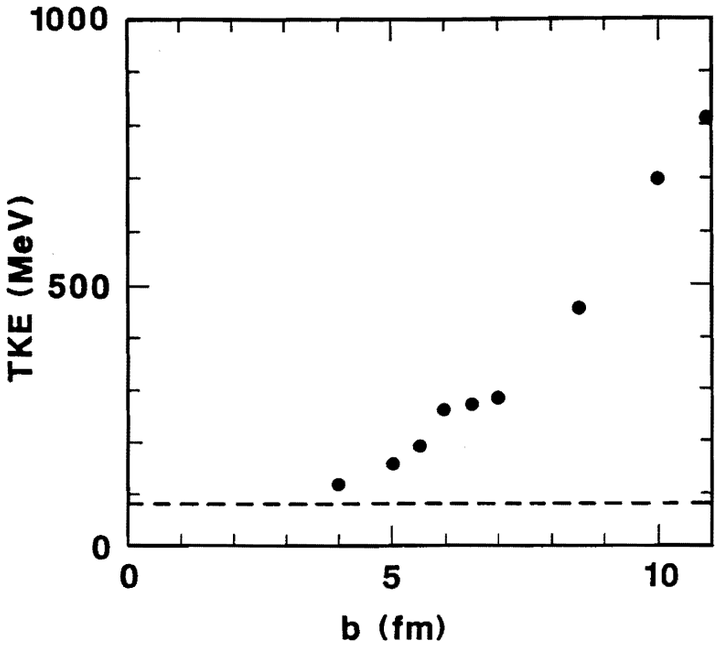

Figure 5

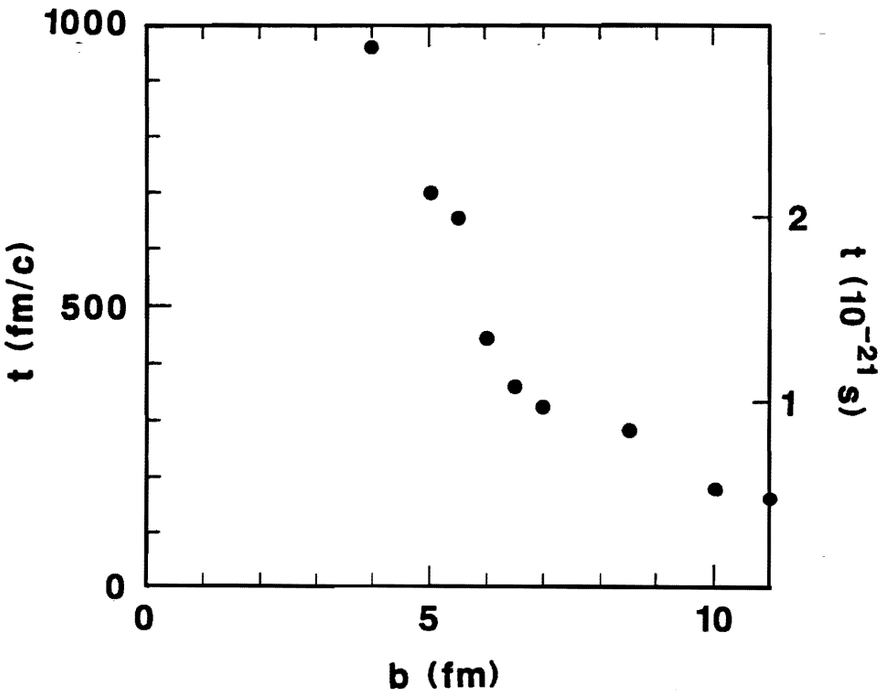

Figure 6

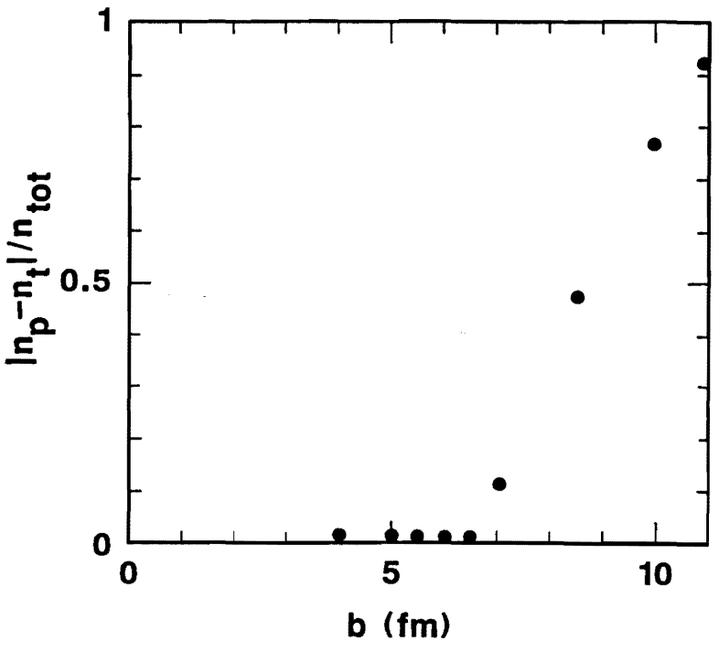

Figure 7

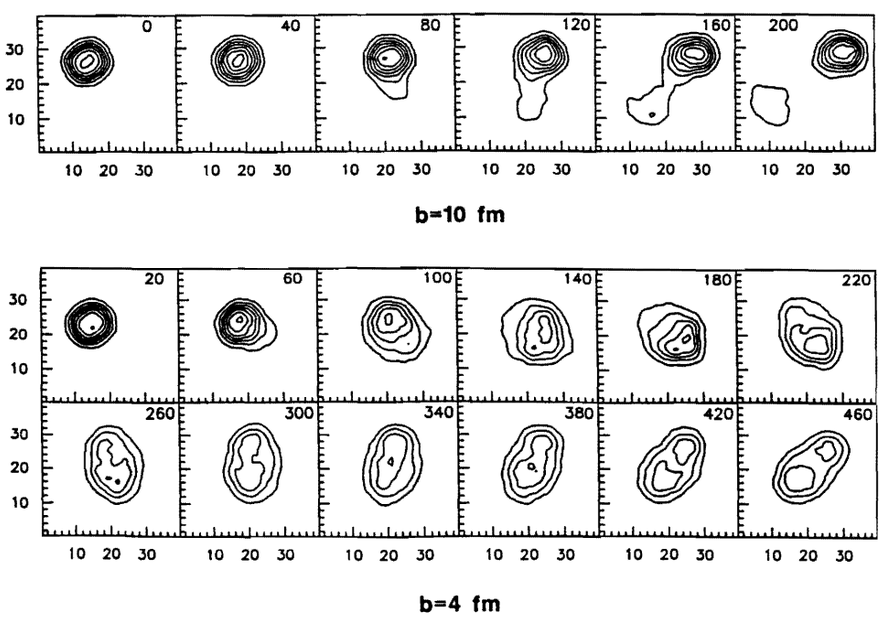

Figure 8

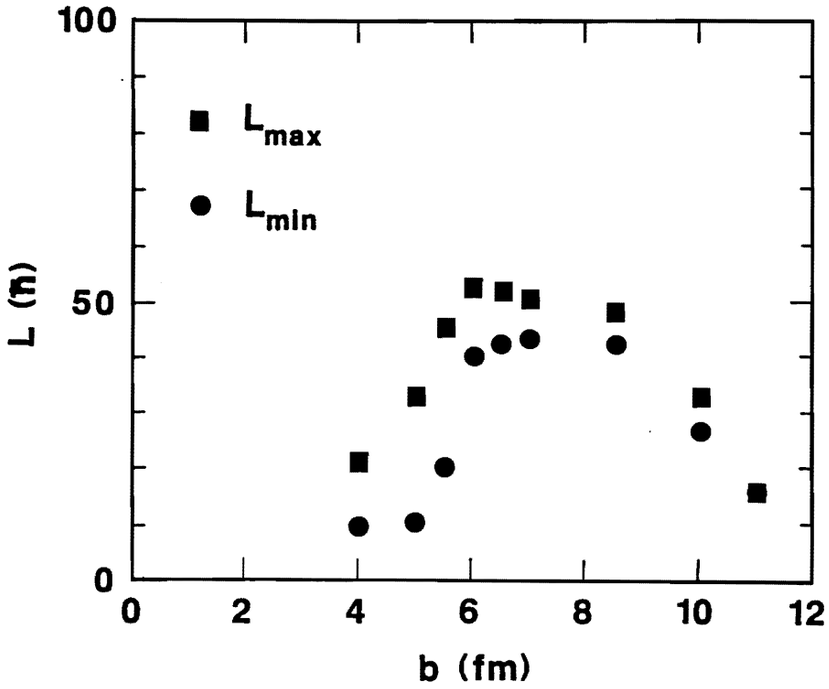

Figure 9

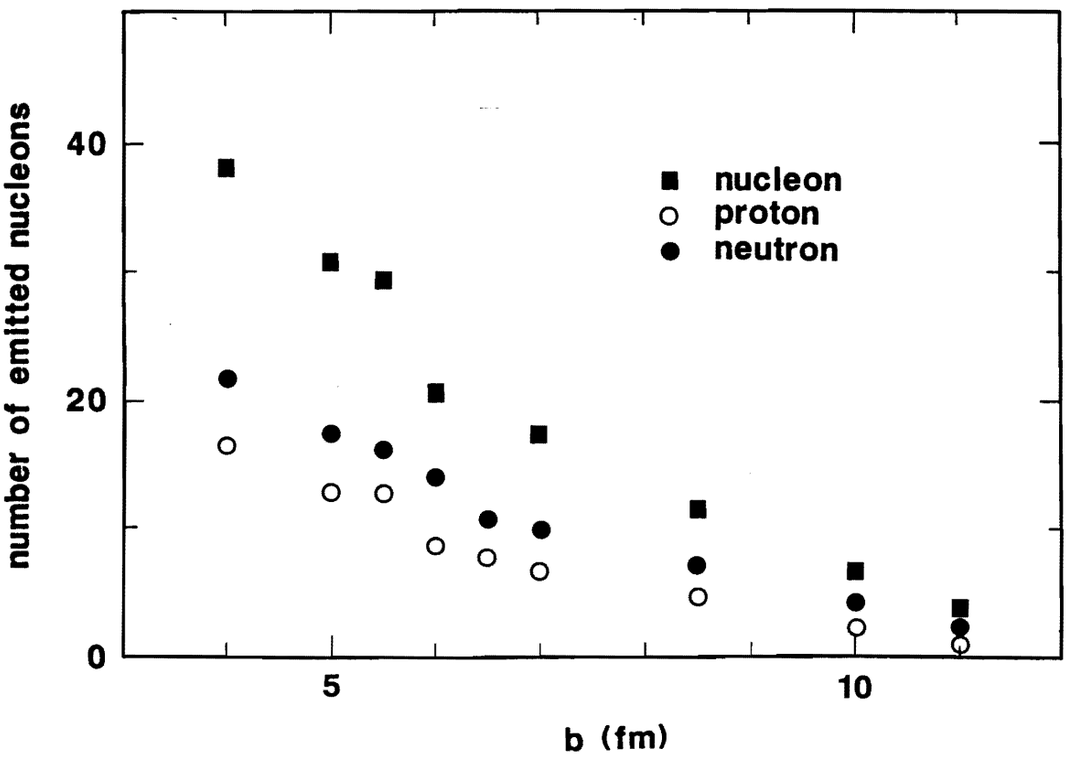

Figure 10

Figure 11

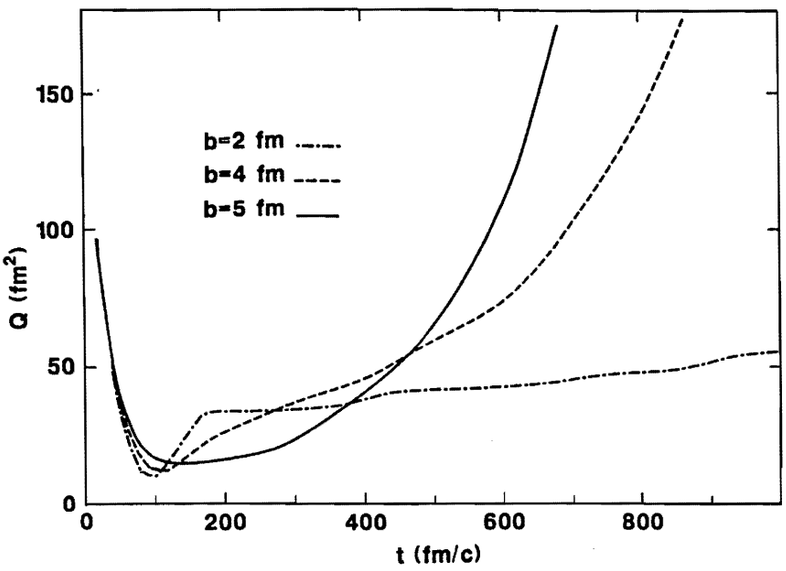

Figure 12a

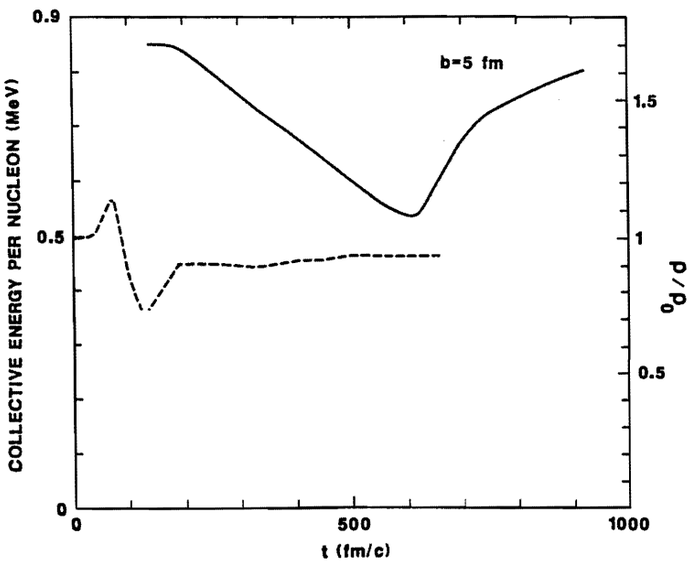

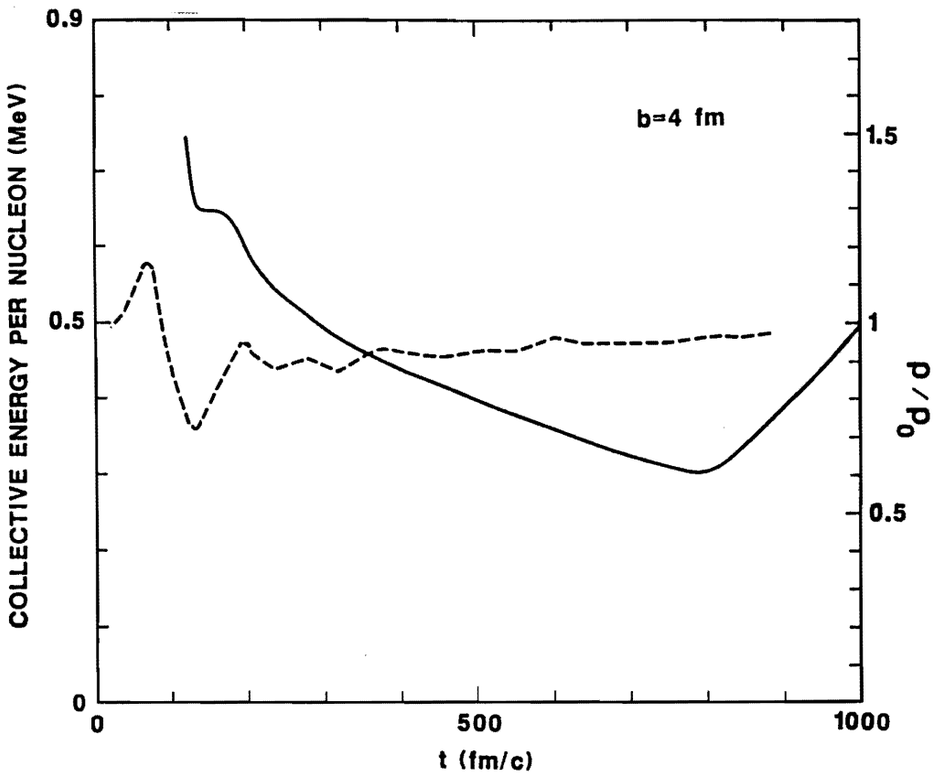

Figure 12b

Figure 12c

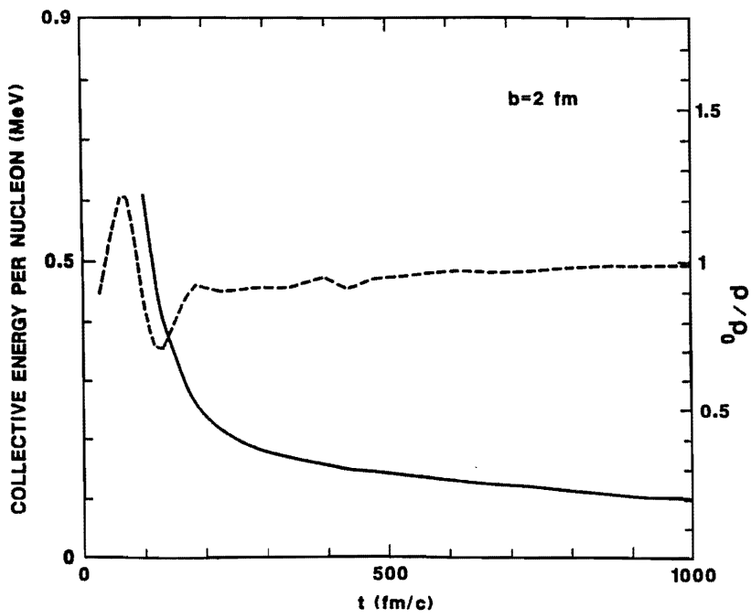

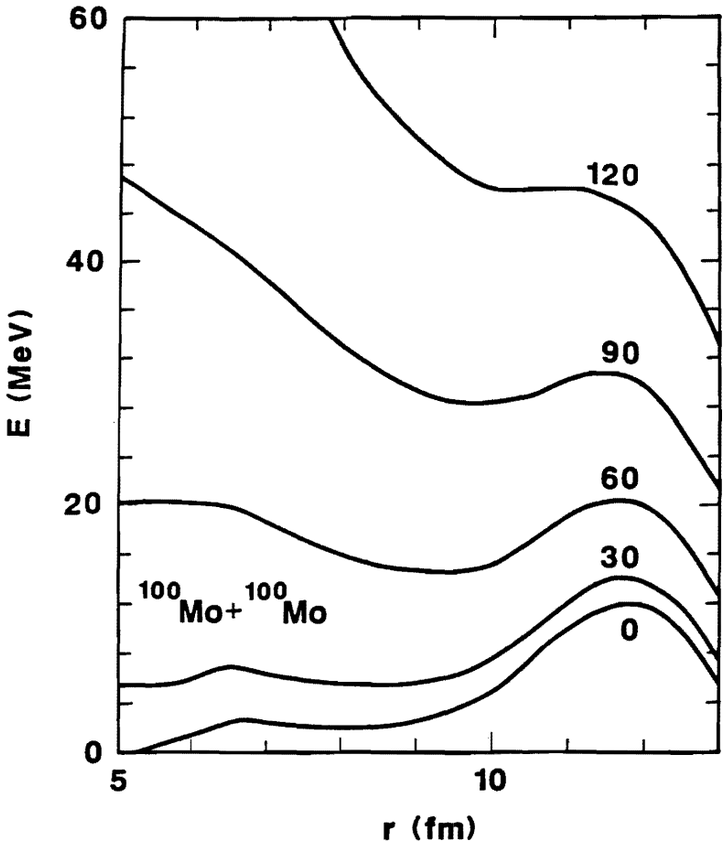

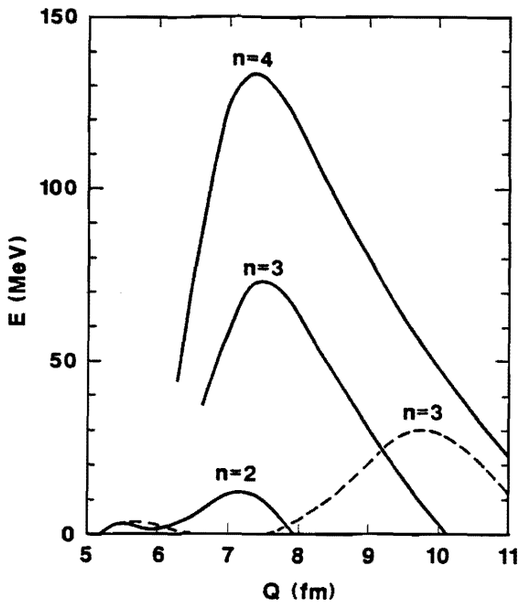

Figure 14

Figure 13

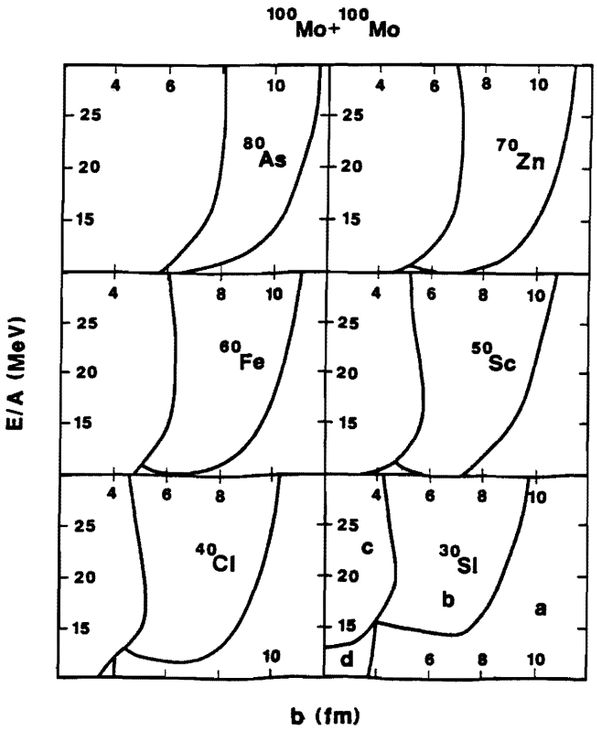

Figure 15